

NOZZLE WEAR IN ABRASIVE JET MACHINING

A Thesis Submitted
in Partial Fulfilment of the Requirements
for the Degree of
MASTER OF TECHNOLOGY

by
RAKESH KUMAR

to the

DEPARTMENT OF MECHANICAL ENGINEERING
INDIAN INSTITUTE OF TECHNOLOGY KANPUR
JUNE, 1982

12345

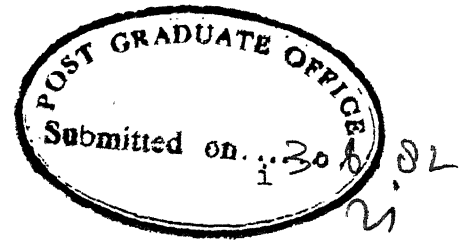
TO
MY LOVING
PARENTS

JUN 1984

CENTRAL LIBRARY

Acc. No. **A 82651**

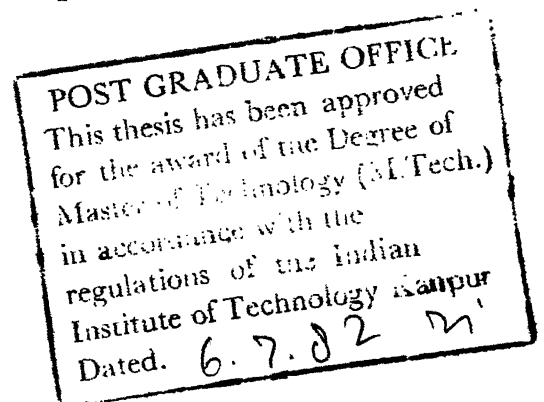
ME-1982-m-kvm-NoZ



CERTIFICATE

This is to certify that the work entitled
" Nozzle Wear in Abrasive Jet Machining " has been
carried out under my supervision and has not been
submitted elsewhere for the award of a degree.

G.K. Lal
Professor
Department of Mechanical Engg.
Indian Institute of Technology,
Kanpur.



ACKNOWLEDGEMENT

I take this opportunity to express my deep sense of gratitude and sincere thanks for the invaluable assistance, that I have received at the worthy hands of my learned guide Dr. G.K. Lal, and for his continued interest in imparting me proper and useful guidance.

I am extremely thankful to Mr. A.P. Verma for devoting his valuable time for very useful discussions and timely guidance at various stages.

I acknowledge with grateful thanks for invaluable cooperation and help which I have received from M/s B.P. Bhartiya, J. Singh, R.M. Jha, O.P. Bajaj and my loving friends.

In the end I wish to put my thanks to Mr. D.P. Saini for his flawless typing.

RAKESH KUMAR

CONTENTS

	<u>Page</u>
CERTIFICATE	i
ACKNOWLEDGEMENT	ii
LIST OF FIGURES	v
LIST OF SYMBOLS	vii
SYNOPSIS	ix
 CHAPTER I - INTRODUCTION AND LITERATURE REVIEW	
I.1: Need for New Technology processes	1
I.2: Abrasive Jet Machining	3
I.3: Erosion Models	6
I.3.1: Finnie's Model	8
I.3.2: J.G.A. Bitter's Model	11
I.3.3: Nielson and Gilcrists Model.	13
I.4: Present Work	15
 CHAPTER II - EXPERIMENTS	
II.1: Set up	16
II.2: Preliminary Experiments and Measurements	17
II.3: Experimental Conditions	20
 CHAPTER III - RESULTS AND DISCUSSIONS	
III.1: Experimental Results	21
III.2: Discussions	23

CHAPTER IV	- CONCLUSIONS AND SCOPE FOR FURTHER RESEARCH	28
APPENDIX	-	30
REFERENCES	-	31

LIST OF FIGURES

<u>FIGURE NO.</u>	<u>DESCRIPTION</u>	<u>PAGE</u>
FIG. 1	Idealized Picture of Abrasive Grain Striking a Surface.	33
FIG. 2	Predicted Variation of Volume with Angle for a Single Abrasive Grain.	33
FIG. 3	Schematic Layout of Abrasive Jet Machine.	34
FIG. 4	Feeder Characteristics.	35
FIG. 5	Experimental Setup (Photographic view).	36
FIG. 6	Successive Wear Profile of the Nozzle.	37
FIG. 7	Tests on Split Nozzle.	38
FIG. 8	Flowmeter Calibration Chart	39
FIG. 9	Variation of Diametral Wear Rate at Different Nozzle Sections	40
FIG.10	Typical Photographs Showing Nozzle Wear.	41
FIG.11(a)	Variation of Wear Index with Time for Different Nozzle Lengths.	43
FIG.11(b)	Variation of Wear Index with Nozzle Length.	44

FIG. 12(a)	Variation of Wear Index with Time for Different Nozzle Diameters.	45
FIG. 12(b)	Variation of Wear Index with Nozzle Diameter.	46
FIG. 13	Variation of Wear Index with Time for Different Nozzle Entrance Angles.	47
FIG. 14(a)	Variation of Wear Index with Time for Different Mixture Ratios.	48
FIG. 14(b)	Variation of Wear Index with Mixture Ratio.	49
FIG. 15	Variation of Wear Index with Time for Different Mesh Size.	50
FIG. 16	Velocity Profile Inside the Nozzle.	51

LIST OF SYMBOLS

- K - Ratio of the vertical force component on the particle face to the horizontal force component
- l - Depth of contact of particle
- y_t - Depth of cut
- Ψ - Ratio of l and y
- α - Angle of attack
- W - Volume of material removed
- m - Mass of single abrasive grain
- V - Velocity of abrasive particle
- M - Mass of many grains
- p - Plastic flow stress
- σ - Shear stress of target material
- V_1 - Particle velocity normal to the body surface
- V_{11} - Particle velocity parallel to the body surface
- X - Maximum particle velocity at which the collision still is purely elastic
- V_{11} - Residual horizontal velocity component

- W_D - Deformation wear
- W_C - Cutting wear
- β - Cutting wear parameter
- λ - Deformation wear parameter
- W^* - Wear Index
- W_d^* - Diametral wear rate

SYNOPSIS

Abrasive Jet Machining is a useful process for micro-drilling of brittle and hard materials, etching of glass surfaces, deburring, polishing etc. In this process material removal from the workpiece takes place due to impact of fine grain abrasive particles carried in a fluid stream. The mixture of abrasive particles and carrier gas is directed to the work surface in the form of a jet by means of a suitably designed nozzle. During the process wear occurs on the inside surface of the nozzle. The literature survey reveals that practically nothing is known about the wear aspects of nozzle, which is of considerable importance from the point of view of material removal rate and accuracy.

In the present work an attempt has been made to experimentally study the nozzle wear during Abrasive Jet Machining under various conditions. The nozzle parameters that have been studied are nozzle length, diameter and entrance angle. The other parameters that have been considered are mixture ratio and grain size. All experiments have been carried out on a specially designed Abrasive Jet Machining set-up, where the input parameter could be precisely controlled.

Initial experiments have been carried out using specially made split nozzles so that the wear profile on the inside surface of the nozzles could be examined. The wear profile indicates that the flow passage could be approximated by a truncated cone. All subsequent data regarding wear have therefore, been obtained using the inlet and outlet diameters of the nozzles. Experiments further reveal that the nozzle cross-section remains circular after use although the diameter increases continuously.

The experimental results indicate that the nozzle wear rate increases with increase in nozzle length, decrease in nozzle diameter and entrance angle. Nozzle wear also increases with increase in mixture ratio and size of abrasive particles. These wear values have been evaluated in terms of a nondimensional parameter, "Wear Index". The results obtained have been discussed on the basis of existing erosion models.

CHAPTER - I

INTRODUCTION AND LITERATURE REVIEW

I.1 NEED FOR NEW TECHNOLOGY

Merchant[1] analysed the needs and trends of future manufacturing technology on the basis of past and present manufacturing activities. According to him, the three outstanding needs of future technology are:

- i) Sustained productivity in face of rising strength barrier ;
- ii) Higher accuracy consistent with the increasing demand for closure tolerances, and
- iii) Versatility of automation.

Rising strength barrier poses the most serious problem to the manufacturing engineers. Metallurgists and material scientists are continuously developing newer and larger varieties of materials having diverse properties and increasingly higher strengths a trend away from conventional materials with conventional properties.

In spite of rapid technological advancements in the field of conventional machining, the machining of carbides and other hard-to-machine materials has been

limited to diamond wheel grinding for a long time. The process has become costly because of the scarcity and high cost of the abrasives necessary for the diamond wheels. Besides, the rapid development of industries like aerospace, nuclear power etc. has been accompanied by an ever increasing use of high strength temperature resistant alloys. The processings of the parts of complicated shapes have also been difficult, time consuming and uneconomical by the conventional techniques of machining. Conventional processes are not in a position to meet these challenges posed by the development of new materials.

To meet these challenges several new manufacturing processes have been developed during the last two decades or so. These processes are not affected by hardness, toughness or brittleness of materials, and can produce intricate shapes on any workpiece material by suitable control over the various physical parameters of the processes. The underlying principle of these new technological processes is to apply some sort of energy, namely mechanical, electrical, chemical, thermal, or magnetic, to the workpiece directly and have the desired shape transformation or material removal from the work surface through use of known scientific principles.

One of these new technological processes involves material removal by erosion or abrasion. Erosion of work material necessitates creation of pneumatic or hydraulic pressure and flowing the fluid carrying the abrasive particles. The process employing this mechanism of material removal is the Abrasive Jet Machining (AJM).

I.2 ABRASIVE JET MACHINING

In abrasive jet machining, material removal takes place by the impact of fine grained abrasive particles carried in a fluid stream. The fine grained abrasive powder mixed with air or some other suitable carrier gas at high pressure in suitable proportion is directed in the form of a jet by means of suitably designed nozzle on to the work surface to be machined. The material removal takes place because of erosive action of abrasive particles impacting the work surface at high velocity.

APPLICATIONS

This process has its successful application for:

- 1) Micro-drilling of brittle and hard materials.
- 2) Etching of markings on glass surfaces.
- 3) Cleaning of metallic moulds cavities which otherwise may be inaccessible.
- 4) Deburring and polishing of plastic, nylon and teflon components.

- 5) Removal of flash and parting lines from the injection moulded parts.
- 6) Cutting of thin sectional fragile components made of glass, refractories, ceramics, mica etc.
- 7) Removal of glue and paint from paintings and leather objects.
- 8) Production of high quality surface.
- 9) Reproduction of design on the glass surface with the help of mask made of rubber, copper etc.
- 10) Frosting of the interior surface of glass tubes.

CHARACTERISTICS OF SOME PROCESS PARAMETERS

CARRIER FLUID:

The carrier fluid used in AJM should be non-toxic, cheaply available and capable of being dried and cleaned without any difficulty. The carrier fluid which can be used are air, carbon dioxide, or nitrogen. The air is most widely used because of cheap and easy availability. Even clean, dry shop air can be used after suitable filtering directly from air lines. Low viscous and lighter fluid gives higher material removal rate as compared to heavy gas or fluid.

ABRASIVE:

The choice for abrasive type depends upon the type of machining (rough or finishing), cost, material

of the workpiece and type of operation. The abrasive powder should be sharp to have better cutting action and fine enough to remain in suspension in the carrier fluid. For cutting purposes aluminium oxide and silicon carbide abrasive powders are generally used, while dolomite, glass beads etc. are used for deburring, polishing and cleaning.

The nozzle wear rate in abrasive jet machining depends upon the grain size and shape of the abrasive powder. Coarse grain abrasives have better cutting action compared to fine grains. Fine grain abrasives have sticking characteristics and tend to make the flow irregular and have choking action in the nozzle and the flow system. The most favourable size for AJM is in the range 10 to 50 μm . Finer grains give better surface finish and hence recommended for polishing or finishing operations.

NOZZLE:

The nozzle used in AJM imparts high velocity to the carrier fluid and thereby to the abrasive particles. Thus the nozzle has to withstand erosive action and must be made of high wear resistant materials. The common materials for nozzles are sapphire and tungsten carbide. The fluid particles having smaller

inertia accelerate faster than the abrasive particles which have comparatively high inertia. Thus the entrance angle of the nozzle should be small and the length should be large to enable the carrier fluid to have sufficient time to impart the momentum to abrasive particles. On the other hand, larger length and smaller entrance angle will cause increased nozzle wear.

Literature review reveals that practically nothing is known about nozzle wear in Abrasive Jet Machining. However, the erosion models proposed by various workers can be helpful in understanding the wear phenomena inside the nozzle. Some of the important erosion models are summarized below.

I.3 EROSION MODELS

In many applications a surface is attacked by solid particles entrained in a fluid stream. This type of wear is generally described as erosion. Probably the most important erosion problems which occur in industry are those connected with the equipment used in the catalytic cracking of oil. However, erosion is also a continuing problem in such units as coal turbines, hydraulic turbines, coal hydrogenation equipment, rocket nozzles and helicopter engines, while usually considered

undesirable, erosion has useful application in such processes as sand blasting, abrasive deburring and erosive drilling of hard materials. Erosion of the nozzle in AJM is also undesirable.

Many studies may be found in the literature of specific erosion problems and their practical solutions. However, the basic principles of this industrially important process have received little attention and is not generally appreciated or understood. There is, in addition, little experimental data in the literature which further limits the possibility of predicting erosion under new and untried circumstances. In particular, the particle velocity, does not seem to have been measured in erosion tests.

The understanding of erosion phenomenon may be divided into two major parts. The first part involves the determination from the fluid flow conditions, the number, direction and velocity of the particles striking the surface. With such information available, the second part of the problem is the estimation of the amount of surface material removed. The first part of the problem is, basically a two phase fluid flow problem and is beyond the scope of the present work. The discussion will therefore, be confined to the mechanism of material removed or erosion rate.

A review of literature reveals that it is unlikely that one mechanism of material removal will apply to all types of materials. For the purpose of understanding, it seems convenient to limit the discussion to two main types of material behaviour, ductile and brittle.

I.3.1 FINNIE'S MODEL

Finnie [2] has proposed a model for erosion of a ductile material when a large number of irregular shaped particles strike the surface. The crater or scratch left by an impacting particle is the first clue to the manner in which erosion occurs. Particles striking the surface at shallow angles (low values of α in Fig. 1) is the condition of greatest interest. For this case the craters have length/depth ratio of the order of 10:1. This leads to the idealized picture of cutting shown in Fig. 1, in which only the leading face of the particle contacts the surface.

Solution of equation of motion of the particle in Fig. 1 can be obtained and by knowing the path it follows through the surface, the material removed can be predicted. The solution requires the knowledge of the forces acting on the particle. The ratio K of the vertical force component on the particle face to the horizontal force component is generally constant. It is also reasonable to assume that the ratio of the depth of contact (l) to the

depth of cut (y_t) has a constant value Ψ . With these simplifying assumptions it is possible to write down and solve the equations of motion of the particle in the x, y and ϕ directions. The volume of surface material eroded by the particle is then taken as the product of the area swept out by the particle tip and the width of the cutting face. Integrating over the cutting period leads to the following simple expressions for the volume of material removed W by a single abrasive grain of mass m , and velocity V

$$W = \frac{mV^2}{p\Psi K} \left(\sin 2\alpha - \frac{6}{K} \sin^2\alpha \right) ; \tan \alpha < \frac{K}{6} \quad \dots \quad (1.1)$$

and

$$W = \frac{mV^2}{p\Psi K} \left(\frac{K \cos^2\alpha}{6} \right) ; \tan \alpha > \frac{K}{6} \quad (1.2)$$

where p is the flow stress of material impacted.

These two expressions predict the same weight loss when $\tan 2\alpha = K/6$. Equation (1.1) applies for lower angles while equation (1.2) applies for higher angles.

The manner in which the predicted volume removal varies with angle α is shown in Fig. 2, for the case $K = 2$. To extend the analysis to multiple particle impact, the mass of a single grain is replaced by M , the mass of many grains. Finnie took 50% off the predicted erosion to allow

for the fact that many particles will not be as effective as the ideal particle. The only remaining unknown is the ratio Ψ ($1/y_t$) and by analogy to metal cutting experiments [3], Ψ can taken to be 2. The volume removal due to a mass M of angular abrasive grains can now be obtained as

$$W \approx \frac{MV^2}{8p} [\sin 2 \alpha - 3 \sin^2 \alpha] ; \alpha < 18.5 \quad (1.3)$$

and

$$W \approx \frac{MV^2}{24p} [\cos^2 \alpha] ; \alpha > 18.5 \quad (1.4)$$

These equations greatly underestimate the weight loss for angles above 45° . Maximum erosion is obtained when $\alpha = 15^\circ - 20^\circ$ and the volume removal in this case can be evaluated from

$$W = 0.075 \left(\frac{MV^2}{2} \right) \frac{1}{p} \quad (1.5)$$

Finnie and Coworkers [4] have proposed that volume loss per individual abrasive particle collision is directly proportional to the total available K.E. of the particle (MV^2) and inversely proportional to the minimum flow or shear stress (σ) of the target material. Their expressions for erosion loss for ductile and brittle materials are

$$\text{Erosion loss} = C f(\alpha) \frac{MV^2}{\sigma} \quad (1.6)$$

and

$$\text{Erosion loss} = C f(\alpha) \frac{MV^{3.3 \text{ to } 6.5}}{\sigma}, \quad (1.7)$$

respectively.

The influence of impingement angle was indicated but not defined mathematically. For better co-relation with experimental results, Bitter[5,6] and Neilson and Gilchrist[7] have modified Finnie's original equations.

I.3.2 BITTER'S MODEL

In erosion two types of wear are involved viz. wear due to repeated deformation (W_D) and cutting wear (W_C). For deformation wear the following equation was found to be satisfactory:

$$W_D = \frac{\frac{1}{2} M [V \sin \alpha - X]^2}{\lambda} \quad (1.8)$$

where X is a constant which can be evaluated from the mechanical and physical properties and λ represents the energy needed to remove a unit volume of material from the body surface.

The particle velocity can be resolved into two components, one normal to the body surface (V_1) and another parallel to it (V_{11}). As a result of V_1 the particle penetrates into the body while V_{11} gives scratching action.

In this scratch and deformation energy is expended, which is supplied by the inertia of the particle, resulting in a decrease of both the vertical and horizontal velocity components. Now there are two possibilities:

- (a) The particle still has a horizontal velocity component (v_{11}) when it leaves the body surface.
- (b) The horizontal velocity component becomes zero during the collision.

In the first case the energy absorbed in the process of scratching is $\frac{1}{2} m (V_{11}^2 - v_{11}^2)$. The quantity of energy needed to scratch out a unit volume from a surface depends on the mechanical properties of the body, assuming that the particle is not destroyed. This quantity is generally called the cutting wear factor β .

The volume W_{c1} cut from the body surface by a single particle in this case is

$$W_{c1} = \frac{\frac{1}{2} m (V_{11}^2 - v_{11}^2)}{\beta} \quad (1.9)$$

while for the case (b) it is given by

$$W_{c2} = \frac{\frac{1}{2} m V_{11}^2}{\beta} \quad (1.10)$$

when $v_{11} \neq 0$, Bitter gives the cutting wear as

$$W_{c1} = 2 M \frac{C (V \sin \alpha - X)^2}{\sqrt{V \sin \alpha}} \left[V \cos \alpha - \frac{C(V \sin \alpha - X)^2}{\sqrt{V \sin \alpha}} \beta \right] \quad \dots\dots (1.11)$$

and when $V_{11} = 0$, cutting wear equation can be expressed as

$$W_{c2} = \frac{\frac{1}{2} M [V^2 \cos^2 \alpha - X_1 (V \sin \alpha - X)^{3/2}]}{\beta} \quad (1.12)$$

where X_1 is a parameter defined by Bitter [6]. We now have equations (1.8), (1.11) and (1.12) giving erosion. The total wear (W_t) at every instant is therefore,

$$= W_D + W_{c1} \quad (1.13)$$

$$= W_D + W_{c2}$$

I.3.3 NEILSON AND GILCHRIST MODEL

According to Neilson and Gilchrist [7], two types of wear takes place. These are deformation wear and cutting wear. If one assumes that for cutting wear $\hat{\lambda}$ units of K.E. must be absorbed by the surface to release one unit mass of eroded material and that the corresponding parameter for deformation wear is λ , then the above factors immediately lead to the following relationships:

$$W = \frac{\frac{1}{2} M (V^2 \cos^2 \alpha - v_{11}^2)}{\beta} + \frac{\frac{1}{2} M (V \sin \alpha - X)^2}{\lambda} ; \alpha < \alpha_0$$

.... (1.13)

and

$$W = \frac{\frac{1}{2} M V^2 (\cos^2 \alpha)}{\beta} + \frac{\frac{1}{2} M (V \sin \alpha - X)^2}{\lambda} ; \alpha > \alpha_0$$

... (1.14)

where X is the velocity component normal to the surface below which no erosion takes place, α_0 is the angle of

attack at which v_{11} is zero. So that at this angle, equations 1.13 and 1.14 predict the same erosion.

These equations are fairly general and the erosion-angle of attack characteristics predicted by them for a particular material depends on the relative magnitudes of cutting and deformation wear constants β and λ when cutting wear predominates X can be neglected which is usually small compared to the particle velocity. For very brittle materials like glass which cannot suffer plastic deformation, the first terms in equations (1.13) and (1.14) do not apply.

I.4 PRESENT WORK

The literature survey reveals that very little is known about erosion of materials and nothing seems to be available on the nozzle wear aspects in AJM. The wear of nozzle is of considerable importance not only from the point of view of cost but also from the point of view of accuracy and material removal rate.

The important parameters affecting wear of nozzle of a given material in AJM appears to be nozzle diameter, nozzle length, nozzle entrance angle, mixture ratio and grain size. In the present work the effect of these parameters have been studied experimentally using a specially designed AJM set-up, where the input parameters could be precisely controlled. The results have been discussed on the basis of existing erosion models.

CHAPTER-II

EXPERIMENTS

II.1 EXPERIMENTAL SET-UP

The experimental set up is shown schematically in Fig. 3. Dry air from the compressor through dehumidifier and filter is allowed to enter the mixing chamber at the regulated pressure. The flow-meter and pressure gauge indicate the flow rate and air pressure of the air entering the mixing chamber. Fine grained abrasive powder stacked in the main abrasive chamber, flows down into the secondary abrasive chamber through a metering tube which maintains a constant head of abrasive. The abrasive powder from the secondary abrasive chamber flows through the abrasive flow metering ventury into the mixing chamber. The abrasive flow from secondary abrasive chamber is controlled by the mechanical vibrator the abrasive flow rate being a function of the amplitude and frequency of vibration. For a given amplitude the abrasive flow rate depends on the frequency of vibration (Fig. 4). By varying the frequency(rpm of motor), the abrasive flow rate in the range of 0.5 to 20 gms/min can be obtained. The mixing

chamber, the secondary abrasive chamber and the main abrasive chamber are maintained at the same pressure through pressure equilizer tubes. Hence, the abrasive flow into the system is not influenced by the pressure and flow rate of air. The system thus provides a controlled air and abrasive mixture into the mixing chamber. The mixture of air and abrasive is directed into the nozzle and appears as a jet at the nozzle out-let tip. The nozzle holder is attached to a hand feed slide for adjusting the nozzle tip distance from the work surface, called the stand-off distance. The workpiece is mounted on a fixture and enclosed in a closed working chamber along with the nozzle and nozzle holder. The working chamber is connected to a vacuum cleaner for removal of abrasive along with the swarf. Photographic view of the complete set up is shown in Fig. 5.

II.2 PRELIMINARY EXPERIMENTS

The set-up was initially operated for a few hours just to check the leakage at various joints. After ensuring no leakage condition, the set-up was used for experiments.

Preliminary experiments were carried out to ascertain the wear rate of the nozzle as well as the wear

profile. For this purpose a set of split nozzles were used. These nozzles were made in two halves and assembled together to get the final profile. Such nozzles could be disassembled after use and inside surface could be examined under a profile projector to obtain the wear profile. During experiments, after an interval of 3 minutes the nozzle wear profile was traced. The inside diameters were measured at a step of 1 mm along the length and diametral wear rate, defined as $(\text{Final dia} - \text{previous dia}) / \text{time}$, was evaluated.

The successive nozzle wear profile is shown in Fig. 6. It is clear that the profile shape of the nozzle very closely resembles a truncated cone. The wear volumes in all subsequent experiments were thus obtained on the basis of the top and bottom nozzle diameters by assuming straight flaring from entry to exit side.

The wear volume was also obtained by weighing the nozzle before and after use. The wear volume thus obtained has been plotted with time in Fig. 7. The wear volume evaluated on the basis of the top and bottom nozzle diameters are also plotted in this figure. It is clear that both the results closely match.

Preliminary experiments were carried out using Aluminium Oxide grains of various mesh sizes ranging from

320 to 600. The most suitable mesh size appeared to be 400. Coarser grains caused damage to the connecting polythene tubes while finer grains often caused choking.

The mixture ratio was kept 0.252 for most of the experiments because of convenience in setting the motor rpm. and air flow rate. The calibration curve of the flow meter is shown in Fig. 8 and procedure for calculation of mixing ratio is given in Appendix I.

The wear profile shown in Fig. 6 clearly indicates that the exit diameter becomes almost 1.3 times the initial exit diameter in 20 minutes. Also the assumption that the wear profile resembles a truncated cone does not appear to be valid after 15 minutes of use. All subsequent experiments were, therefore, carried out upto 15 minutes only. Further, the time interval for recording of successive wear profile was also reduced to 2.5 min.

Typical variations in the diametral wear rate at different nozzle sections during machining are shown in Figure 9. These results have been obtained using split nozzles.

II.3 EXPERIMENTAL CONDITIONS

Experiments have been carried out to study the wear of nozzles in AJM under the following experimental conditions:

NOZZLE

Material : High carbon high chromium die steel
 Hardness : 50 R_C
 Length : 9.16 mm, 10.16 mm, 12.5 mm, 16.13 mm
 Diameter : 0.8 mm, 0.9 mm, 1.17 mm, 1.62 mm
 Entrance Angle : 60°, 90°, 120°

CARRIER FLUID : Air

Inlet Pressure : 3.8 kg/cm²

Flow rate : 3534.863 ml/min

MIXTURE RATIO : 0.096, 0.252, 0.332

ABRASIVE

Type : Al₂O₃

Mesh size : 400 mesh, 500 mesh

CHAPTER-III

EXPERIMENTAL RESULTS AND DISCUSSIONS

III.1 EXPERIMENTAL RESULTS

Nozzle wear experiments have been carried out over the range of experimental conditions indicated earlier. The wear values in these tests have been obtained from the inlet and outlet diameters of the nozzles. Fig. 10 shows some typical shadowgraph pictures of the nozzle diameters. The wear results obtained with nozzles of various sizes and different mixture ratios and grain sizes have been plotted in Figures 11 to 15.

Nozzle wear has been evaluated in terms of wear volume. The wear rate is thus a function of the length and the diameter of the nozzle. These parameters not only influence the wear volume but also influence the wear rate. Since they affect the flow pattern of the particles inside the nozzle in terms of velocity and pressure. For the purpose of comparing the performance of nozzles of various sizes, the nozzle wear in Figures 11 to 15 have been plotted in terms of a nondimensional parameter, wear Index (w^*) defined as

$$w^* \text{ (wear Index)} = \frac{\text{Final volume of the flow passage} - \text{Initial volume of the flow passage}}{\text{Initial volume of the flow passage}}$$

In Fig. 11(a) the variation in wear Index with time has been plotted for nozzles of various lengths. The general pattern of the curve is almost same in all the cases with wear Index initially increasing linearly and then tending to saturate. As expected, wear rate increases when nozzle length is increased Fig. 11(b). Similarly Fig. 12(a) indicates how the wear Index varies when nozzles of different diameters are used. Fig. 12(b) clearly indicates that the wear rate decreases with increase in nozzle diameter.

Figure 13 indicates the variation of wear Index with time for different nozzle entrance angles. Here also the initial wear rate is high but it tends to saturate soon. Further, the wear rate increases when the nozzle entrance angle is decreased.

Figure 14(a) indicates that with increasing mixture ratio the wear rate increases. Initially, the curve is linear and then tends to saturate.

The effect of grain size is shown in Fig. 15. Tests with grains of mesh sizes 400 and 500 indicate that larger grains cause increased wear. The general pattern of the curves are similar to ones obtained in Fig. 14.

III. 2 DISCUSSION

The wear of nozzle is due to erosion of inside surface by the abrasive particles suspended in the air stream. As discussed earlier, the erosion rate is a function of impinging velocity, particle size and the impingement angle. Further, the mechanism of material removal will depend upon the material of the surface of impingement.

Suspended particulated flow is very complex but a simplified treatment may be considered on the basis of one dimensional steady-state flow of a single particle in a nozzle of fixed geometry. This would provide some insight regarding the velocity of the abrasive particle within the nozzle.

The motion of a small particle suspended in a turbulent fluid was formulated by Corrosin and Lumley [13]. As a simplified approach one could consider only the inertia and drag forces of a single spherical particle suspended in the fluid stream. The motion equations for this situation has been written [14] as

$$U'_p \frac{dU'_p}{dx} = \frac{3}{4} \frac{\mu_g R_e C_d}{d_p^2 \rho_p U_{g1}} (U'_g - U'_p) \quad (3.1) \quad 24$$

and

$$U'_g = \left[1 + \frac{2}{(\nu-1)M_1^2} \right] U_g^{\nu+1} - \frac{2}{(\nu-1)M_1^2 \left(1 - \frac{x}{r_1} \tan \frac{\theta}{2}\right)^{2\nu-2}} \frac{1}{\nu+1} \quad \dots (3.2)$$

where

$$U'_p = \frac{U_p}{U_{g1}}, \quad U'_g = \frac{U_g}{U_{g1}} \text{ and } M_1 = \frac{U_{g1}}{\sqrt{\gamma R T_1}}$$

Here U'_p and U'_g are non-dimensional particle and gas velocities. μ_g is the viscosity of gas, C_d is the drag coefficient, d_p and ρ_p are the diameter and density of abrasive particle. These equations have been solved numerically and resulting velocity patterns are shown qualitatively in Figure 16.

Fig. 16 clearly shows that the particle velocity within the nozzle increases and is maximum at the nozzle exit. Further, the exit velocity of the suspended particle will increase when the nozzle length is increased. It is also clear that the inertia effects cause the particles to lag behind the carrier gas. With increasing nozzle length, the particle will tend to catch-up with the carrier gas (air) velocity. Since erosion is strongly dependent on the impact velocity [15], the wear within the nozzle must increase continuously from inlet to the exit end. This appears to be the case as shown in Fig. [6].

The particle velocity within the nozzle is also a function of the nozzle diameter. During use, the nozzle diameter increases resulting in decreased particle velocity which in turn will cause a decrease in the wear rate. This is clearly shown in Fig. 11 and 12, where the curves show a decrease in wear rate with time. Initially the wear Index is almost linear and then tends to saturate. This is because initially the wear rate is high and with the increase in nozzle diameter (due to erosion) velocity of the abrasive particle decreases resulting in decreased wear rate.

The effect of nozzle diameter on the wear rate is shown in Fig. 12. The mass flow rate of the air was kept the same in all these cases. The fluid velocity and hence the particle velocity will therefore, be more for smaller diameter nozzles. This, in turn, must cause increased wear rate in smaller diameter nozzles which is the case in Fig. 12.

Fig. 13 indicates the effect of nozzle entrance angle on wear rate. Smaller the entrance angle more will be the wear, since the effective length of the tapered portion of the nozzle increases. Referring to equation (3.2), as θ decreases, the gas velocity and hence the particle velocity increases. Thus wear rate must increase with decrease in the entrance angle.

Mixture ratio is another important parameter in AJM. Fig. 14(a) indicates that the wear rate increases when the mixture ratio is increased. This is obvious from the fact that higher is the mixture ratio, more will be the number of particles impacting over the surface causing increased erosion. The erosion rate is, however, not likely to increase continuously, since the kinetic energy of the carrier gas available for transporting the abrasive particles will tend to decrease with increase in mixture ratio [16]. This is clear from Fig. 14(b).

The effects of grain size on nozzle wear have also been investigated through use of particles of mesh sizes 400 and 500. The erosion of material, as mentioned earlier, is not only a function of the impingement velocity but also the size of the impinging particles. For the same impingement velocity, larger particles will remove more material. However, the inertia of coarser particle is more hence the velocity attained will be less. The number of particles impinging on the surface, for a given mixture ratio, also depends on the particle size. Thus smaller particles will have more impacts but will have smaller eroded particles. The coarser grains, on the other hand, will have fewer impacts but larger eroded particles. Effect of particle size on erosion

rate, therefore, will be a combined function of the velocity, the size of the impacting particle as well as the number of impinging particles. Fig. 15 however shows that the wear rate is higher when larger abrasive particles are used.

CHAPTER-IV

CONCLUSIONS AND SCOPE FOR FURTHER RESEARCH

IV.1 CONCLUSIONS

The experiments conducted with split nozzles clearly indicate that the nozzle wear increases almost linearly from the entry to the exit end. The profile of the flow passage, after wear, closely approximates a truncated cone. Wear volume could thus be estimated with sufficient accuracy on the basis of inlet and exit diameters.

Experiments clearly indicate that nozzle wear increases with increase in nozzle length and decrease in nozzle diameter. Similarly nozzle wear increases when the entrance angle of the nozzle is decreased. Increase in mixture ratio and size of abrasive particle also increase the wear rate.

IV.2 SCOPE FOR FURTHER RESEARCH

Quantitatively the velocity profiles of carrier gas (air) and abrasive particles inside the nozzle can be worked out with the help of equations (3.1) and (3.2)

Knowing the velocity profile at a particular section and using a simplified model of erosion, it is possible to calculate the erosion rate at various sections. The calculated erosion rate can then be verified with the experimental results. Such an analysis would be useful for designing appropriate nozzles for AJM.

The work can also be extended to include the effects of nozzle material and grain type.

APPENDIX - I

CALCULATION OF MIXTURE RATIO

The manufacturers calibration for the flow meter indicates that 1 div (1 mm) = 45.9073 ml/min of air. During the experiments the flow meter reading was maintained at 60 and the calibration chart Fig. 8 gives the rate of air supply

$$= 3534.863 \text{ ml/min}$$

The air density is given by

$$\rho = \frac{.001293}{(1+.00367t)} \left(\frac{H}{76} \right) \quad (1)$$

where H is the height of Hg in cms and t is the temperature in °C. The pressure gauge reading in all cases was maintained at 54 psi or 6° .7 absolute.

Therefore,

$$\begin{aligned} \rho &= \frac{.001293}{(1+.00367 \times 30)} \left(\frac{355.1836}{76} \right) \\ &= .0054 \text{ gms/min} \end{aligned}$$

and the rate of air supply = 3534.863 X .0054 = 19 gms/min.

The mixture ratio has been defined as

$$\text{M.R} = \frac{\text{abrasive flow rate}}{\text{Air flow rate}}$$

and can be evaluated if abrasive flow rate (gms/min) is known.

REFERENCES

1. Bhattacharyya, A., "New Technology", The Institution of Engineers (India), 1977.
2. Finnie, I., "Erosion of Surfaces by Solid Particles", Wear, Vol. 3, 1960, p. 87.
3. Finnie, I., and Shaw, M.C., "The Friction Process in Metal Cutting", Trans. ASME, Vol. 78, 1956, p. 1649.
4. Smeltzer, C.E. et. al., "Mechanisms of Metal Removal by Impacting Dust Particles", Trans. ASME, J. Basic Engg., Vol. 92, 1970, p. 639.
5. Bitter, J.G.A., "A Study of Erosion Phenomena" Part I Wear, Vol. 6, 1963, p. 5.
6. Bitter, J.G.A., "A Study of Erosion Phenomena" Part II Wear, Vol. 6, 1963, p. 169.
7. Neilson, J.H., and Gilchrist, A., "Erosion by a Stream of Solid Particles", Wear, Vol. 11, 1968, p. 114.
8. Finnie, I., "Some Observations on the Erosion of Ductile Metals", Wear, Vol. 19, 1972, p. 81.

9. Sheldom and Finnie, I., "The Mechanics of Material Removal in the Erosive Cutting of Materials", Trans. ASME, J. of Engg. for Ind., Vol. 88B, p. 393.
10. Lvoie, F.J., "Abrasive Jet Machining", Machine Design, 1973, p. 135.
11. Ingulli, C.N., "Abrasive Jet Machining", Tool and Manufacturing Engineers, Vol. 59, 1967, p.28.
12. Sarkar, P.K. and Pandey, P.C., "Some Investigation on the Abrasive Jet Machining", Paper presented at the semi Annual meeting, Mech. Engg. Division, Inst. of Engineer's (India) Aug., 1975.
13. Corrosin, S. and Lumley, J., "On Equation of Motion for Particle in Turbulent Fluid", Appl. Sci. Res. A., Vol. 6, 1957, p. 114.
14. Verma, A.P., Unpublished work, 1982.
15. Wolak, J., Worm P., Patterson, I. and Bodoia, J., "Parameters Affecting the Velocity of Particles in an Abrasive Jet", Trans. ASME, J. of Engg. Mat. and Tech., Vol. 99, 1977, p. 147.
16. Soo, S.L., "Fluid Dynamics of Multiphase Systems", Blaisdell Publishing Company, U.S.A., 1967.
17. Neilson, J.H. and Gilchrist, A., "Erosion in Rocket Motor Tail Nozzles", Wear, Vol.11, 1968, p. 137.

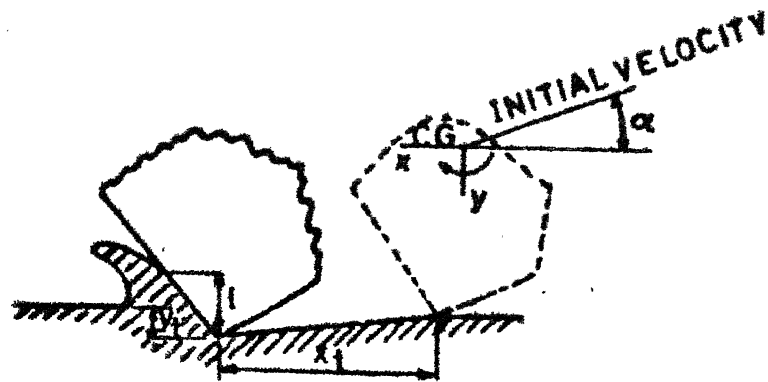


FIG1 IDEALIZED PICTURE OF ABRASIVE GRAIN STRIKING A SURFACE [Ref. 2]

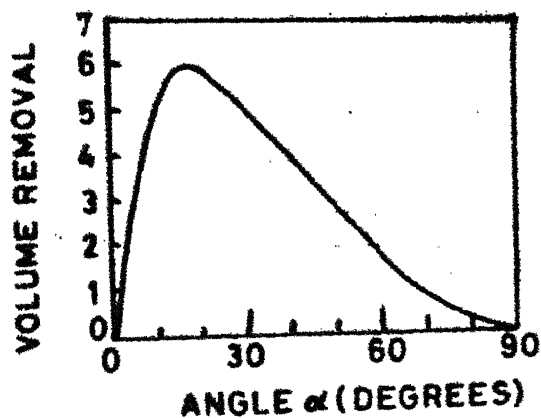


FIG.2 PREDICTED VARIATION OF VOLUME REMOVAL WITH ANGLE FOR A SINGLE ABRASIVE GRAIN [Ref. 2]

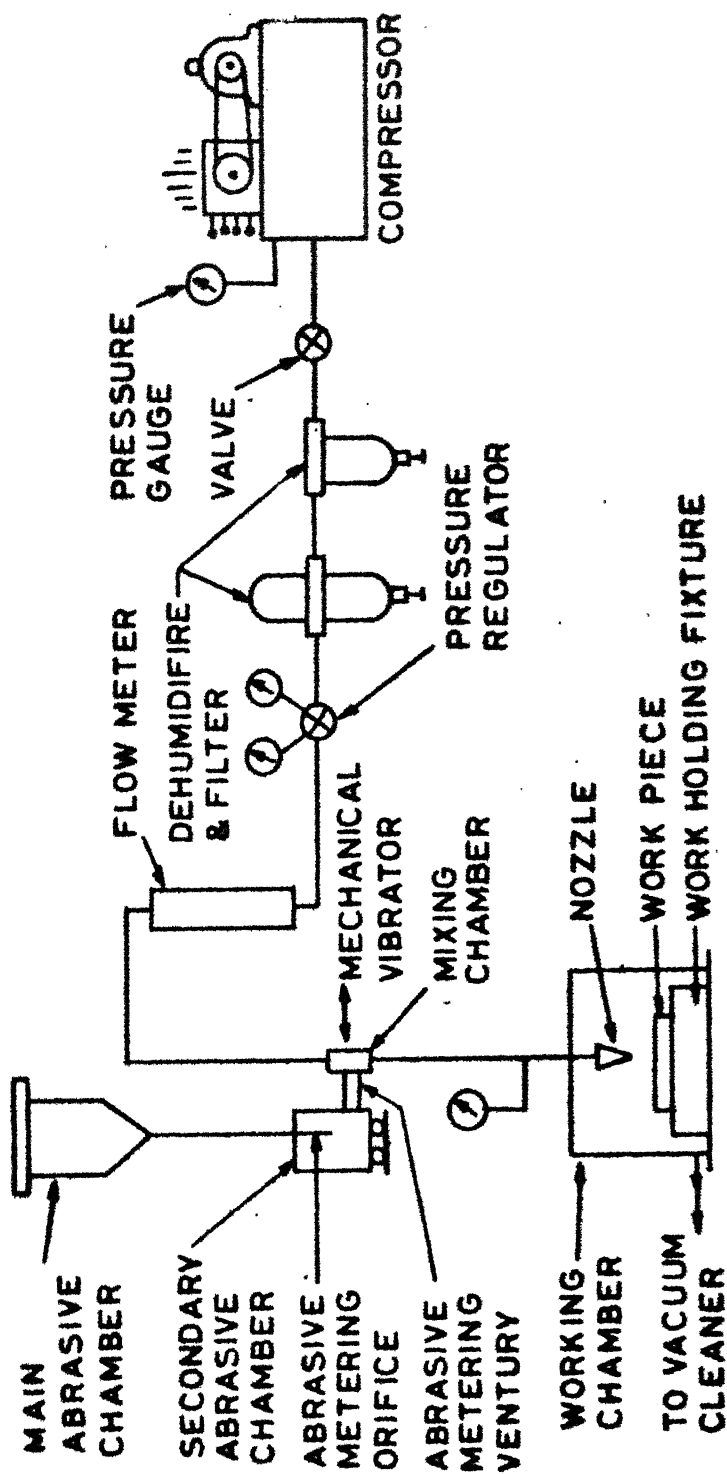


FIG.3 SCHEMATIC LAYOUT OF ABRASIVE JET MACHINE

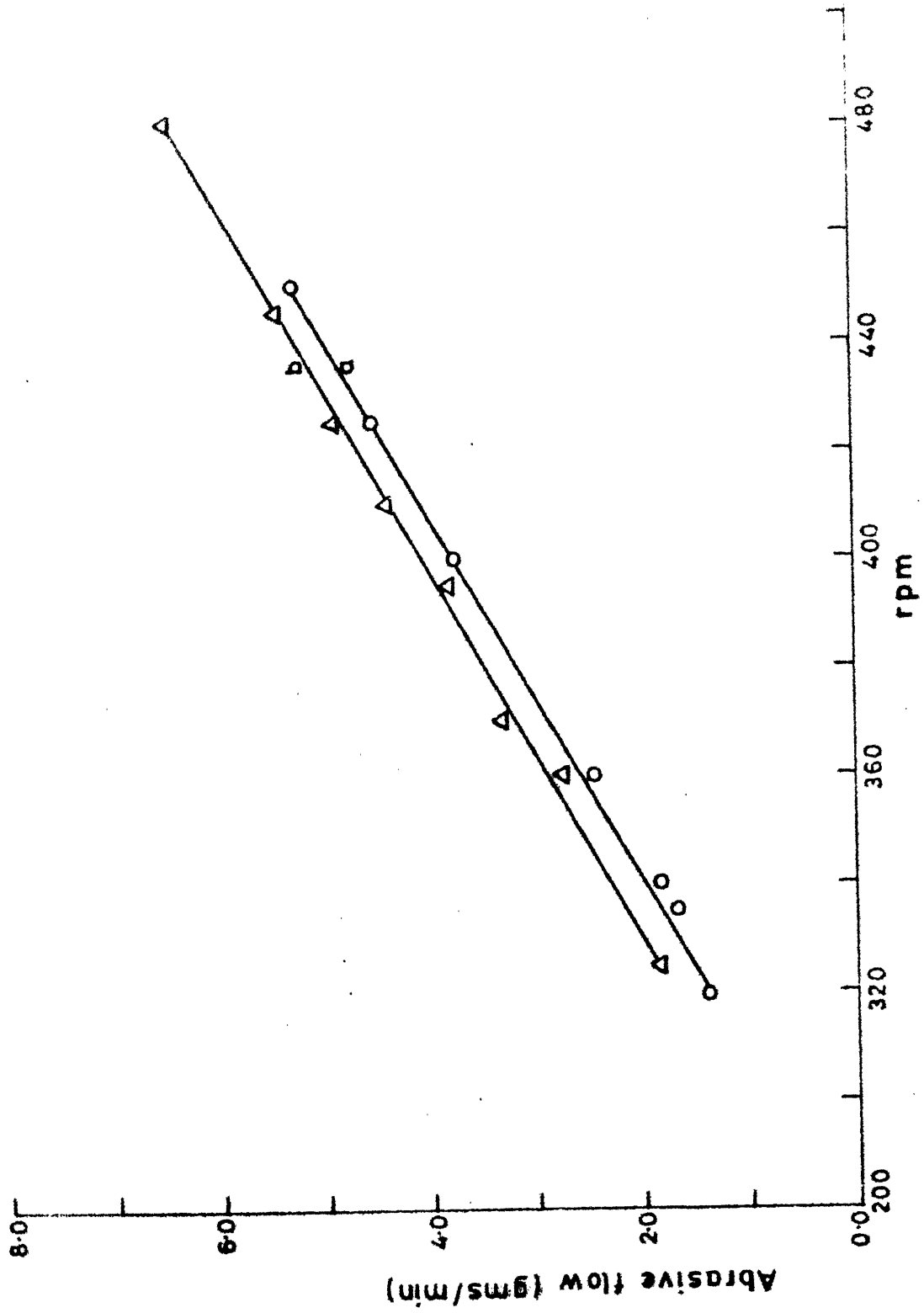


FIG.4 FEEDER CHARACTERISTICS (a) 500 mesh, (b) 400 mesh

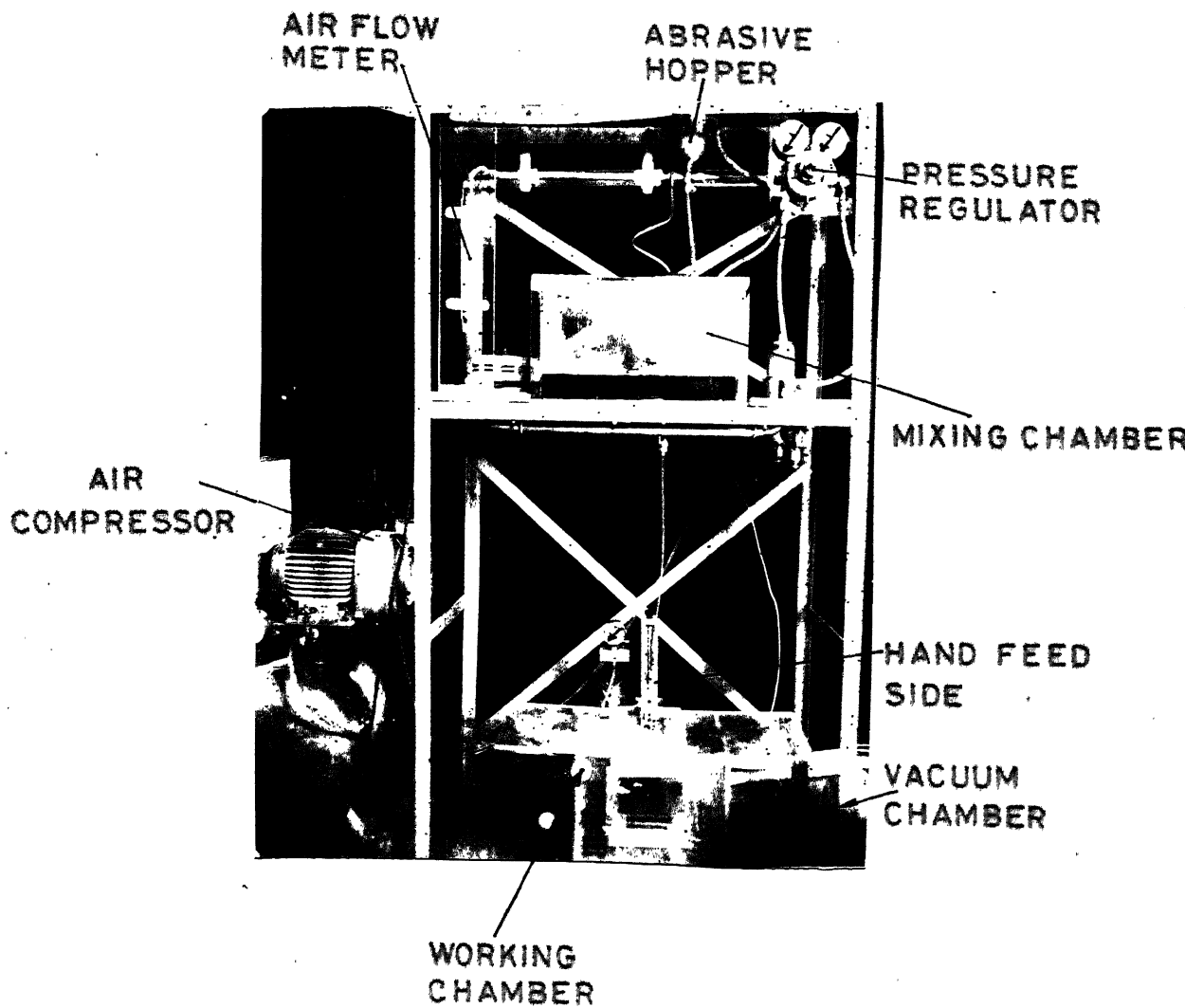
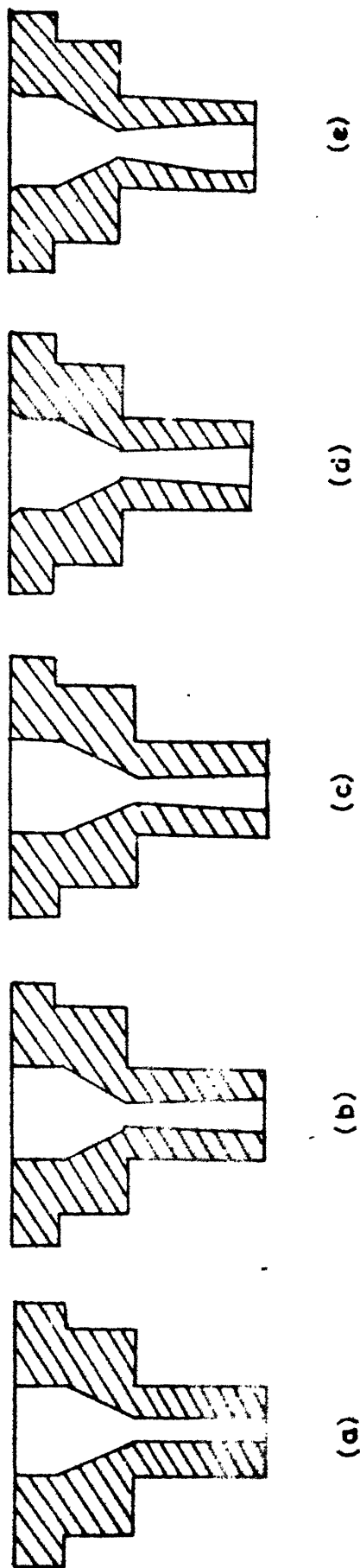


FIG.5 EXPERIMENTAL SETUP



Nozzle dia = 0.78 mm

Nozzle length = 4.5 mm

$\theta = 60^\circ$

Abrasive: 400 mesh; Al_2O_3

Nozzle hardness = 50 Rockwell 'C'

Mixture ratio = 0.252

FIG. 6 SUCCESSIVE WEAR PROFILE OF THE NOZZLE

(a) Initial profile (b) After 5 min (c) After 10 min

(d) After 15 min (e) After 20 min

(shadow graph tracings)

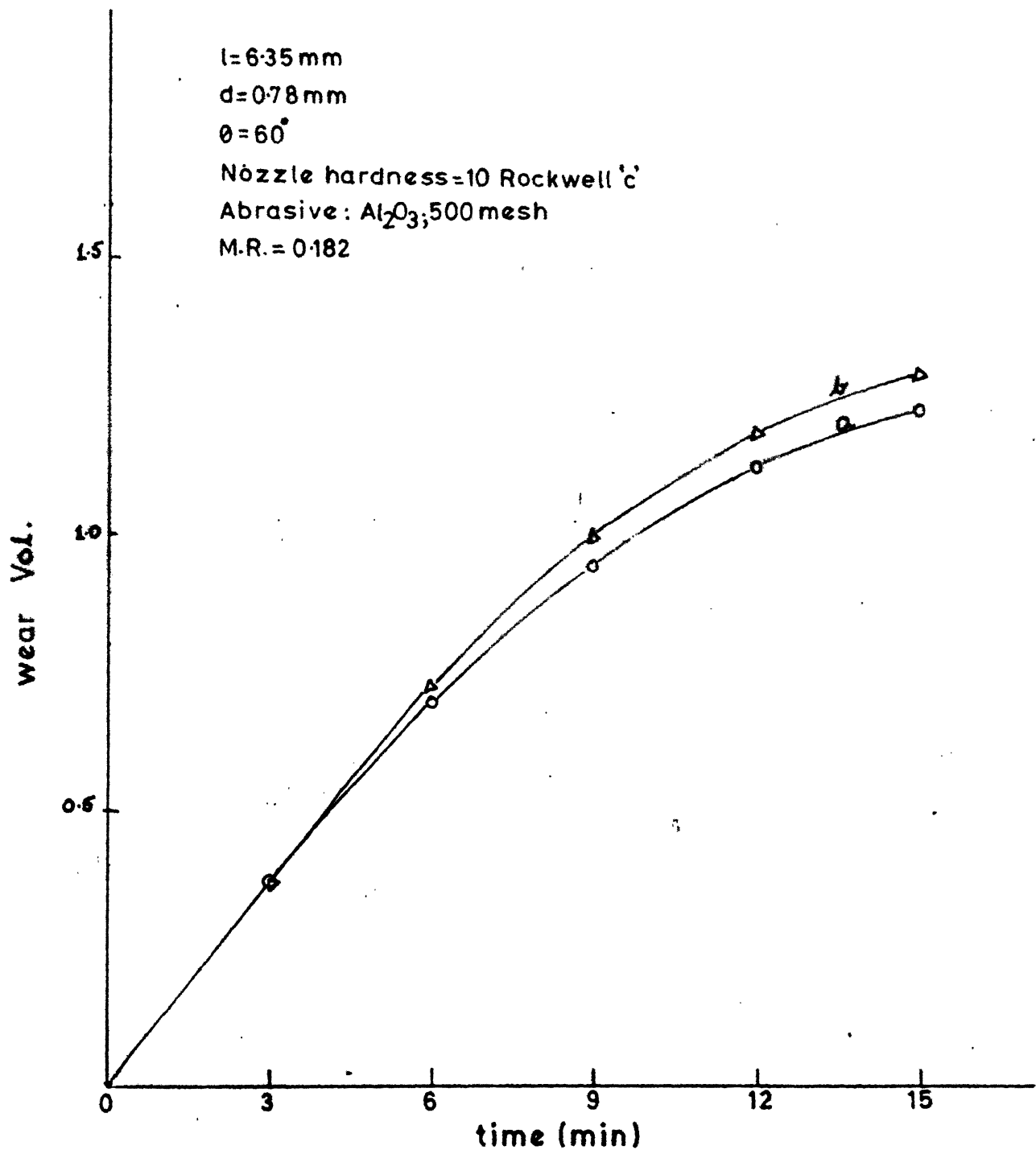


FIG.7 TESTS ON SPLIT NOZZLE

a) Wear vol. obtained from inlet and exit dia.

b) Wear vol. calculated from difference of weight.

SIZE NO. 3

CALIBRATION CHART

R₄ FLOWMETER CATALOG NO. F1300*
STD.
AIR
ML./MIN.

SERIAL NO. _____

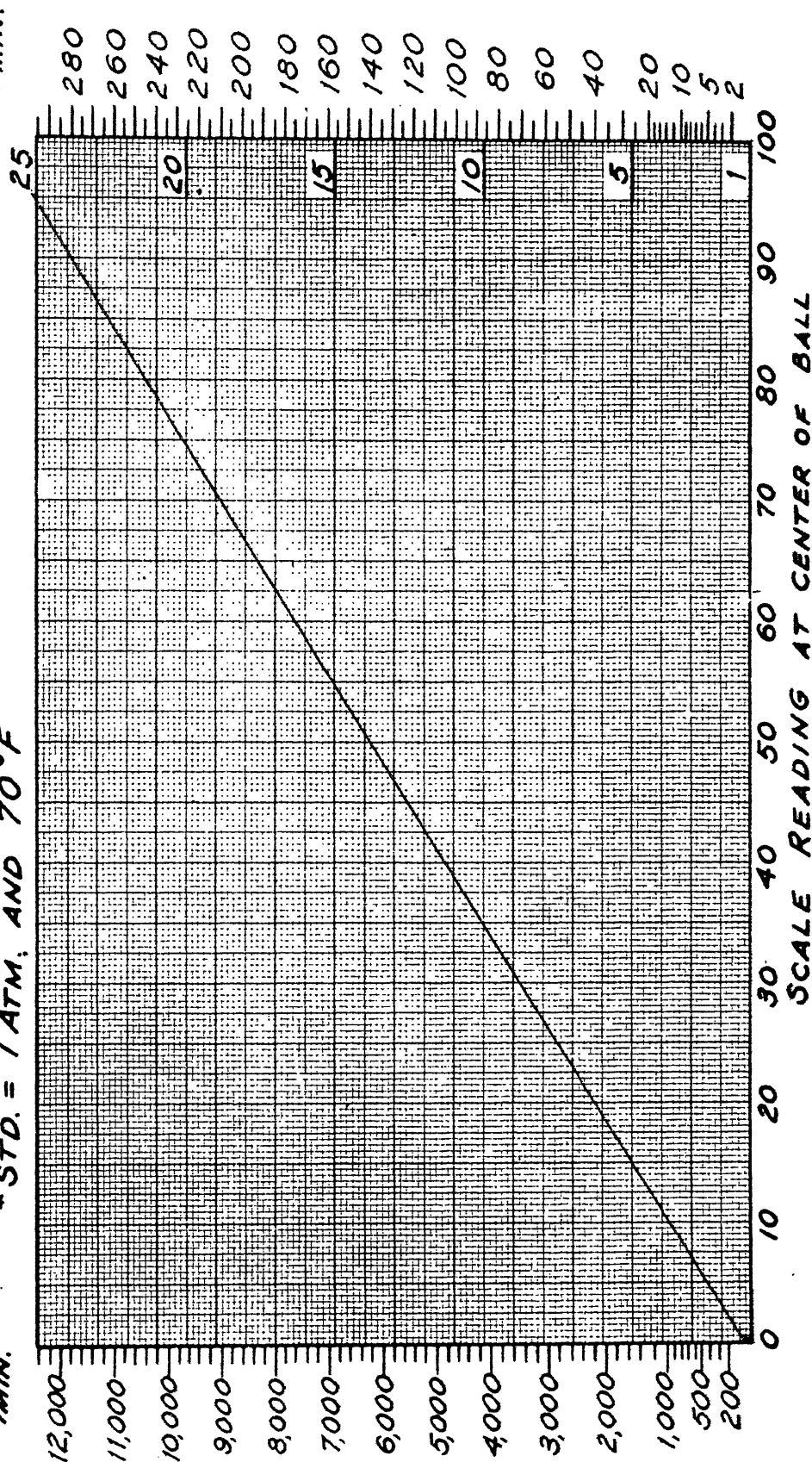
 $D_f = 0.250"$ $W_f = 0.339$ GM. $\rho_f = 2.53$ GM./ML.

*STD. = 1 ATM, AND 70°F.

*
STD.
WATER
ML./MIN.

↑

R



SCALE READING AT CENTER OF BALL

FIG. 0

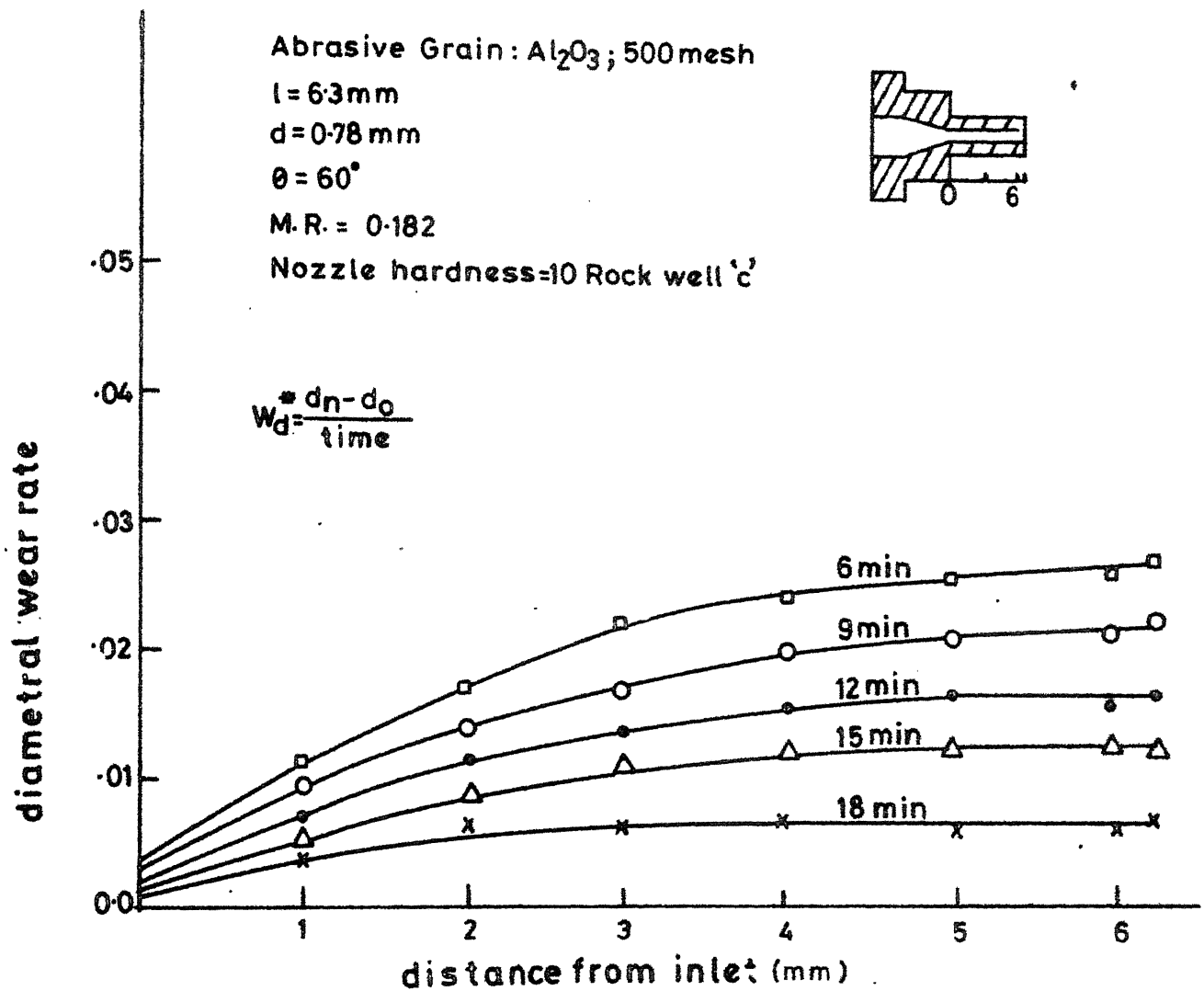
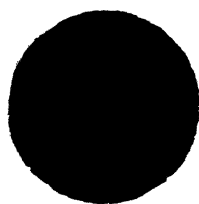
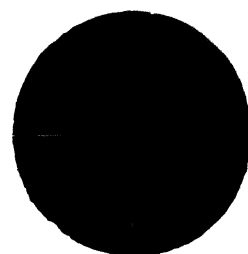


FIG. 9 VARIATION OF DIAMETRAL WEAR RATE AT DIFFERENT NOZZLE SECTIONS

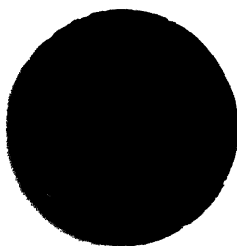


Initial outlet dia
(.8 mm)

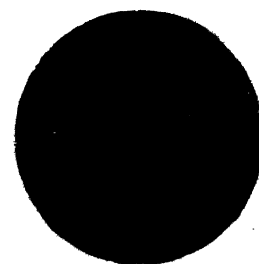


After 15 min
(1.035 mm)

$l = 12 \text{ mm}$, $\theta = 60^\circ$, $M.R = .252$ Abr: Al_2O_3 ; 400 mesh
Magnification = $\times 31\frac{1}{4}$

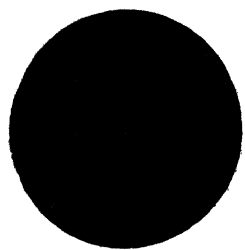


Initial outlet dia of
120° nozzle (.96 mm)

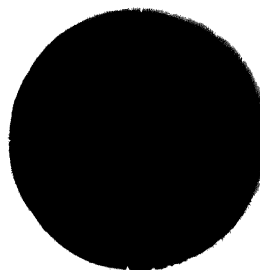


After 15 min
(1.08 mm)

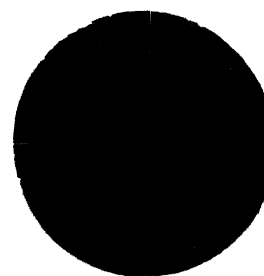
$l = 5.25 \text{ mm}$, $M.R. = .252$, $d = .96 \text{ mm}$ Abr: Al_2O_3 ; 400 mesh
Magnification = $\times 31\frac{1}{4}$



Initial outlet dia
(.97 mm)



After 7.5 min
(1.06 mm)



After 15 min
(1.10 mm)

Abr: Al_2O_3 ; 500 mesh , $l = 8.16 \text{ mm}$, $d = .97 \text{ mm}$, $\theta = 60^\circ$, M.R.= .25

Magnification = X $31\frac{1}{4}$

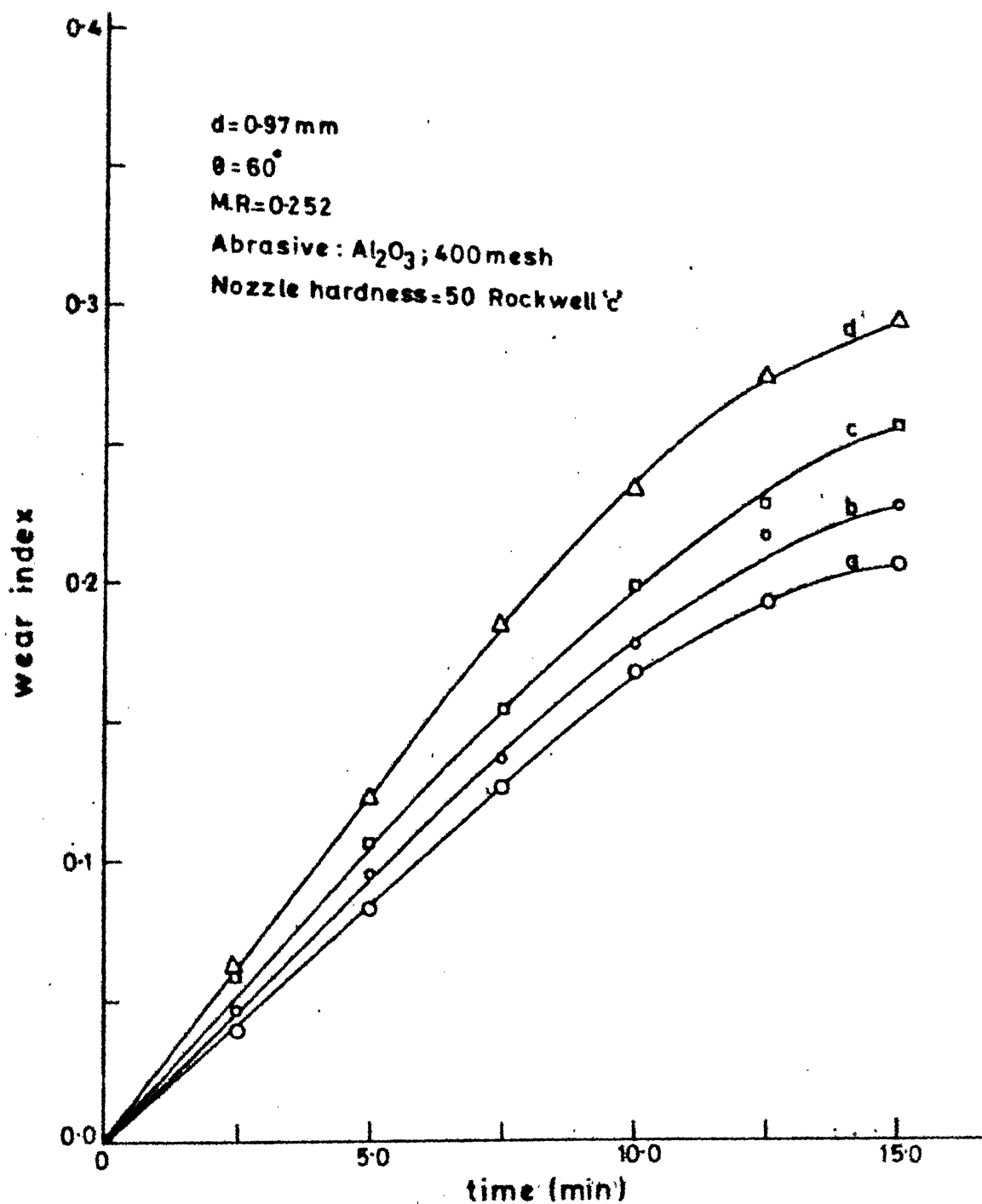


FIG. 11(a) VARIATION OF WEAR INDEX WITH TIME FOR DIFFERENT NOZZLE LENGTHS

(a) $8.41d$ (b) $10.47d$ (c) $12.88d$ (d) $16.68d$

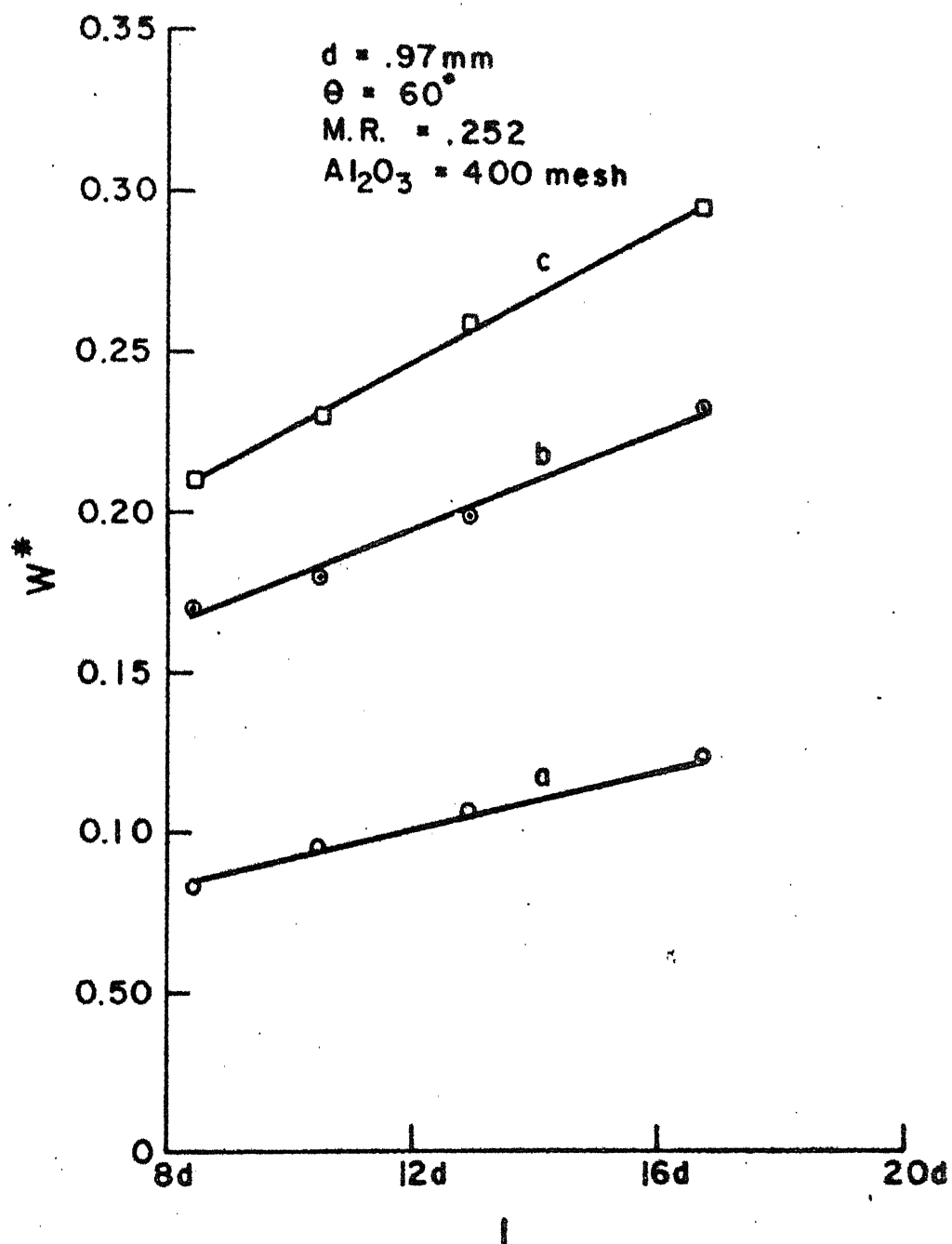


Fig. 11b Variation of wear index with nozzle length (a) for 5 min., (b) for 10 min., (c) for 15 min.

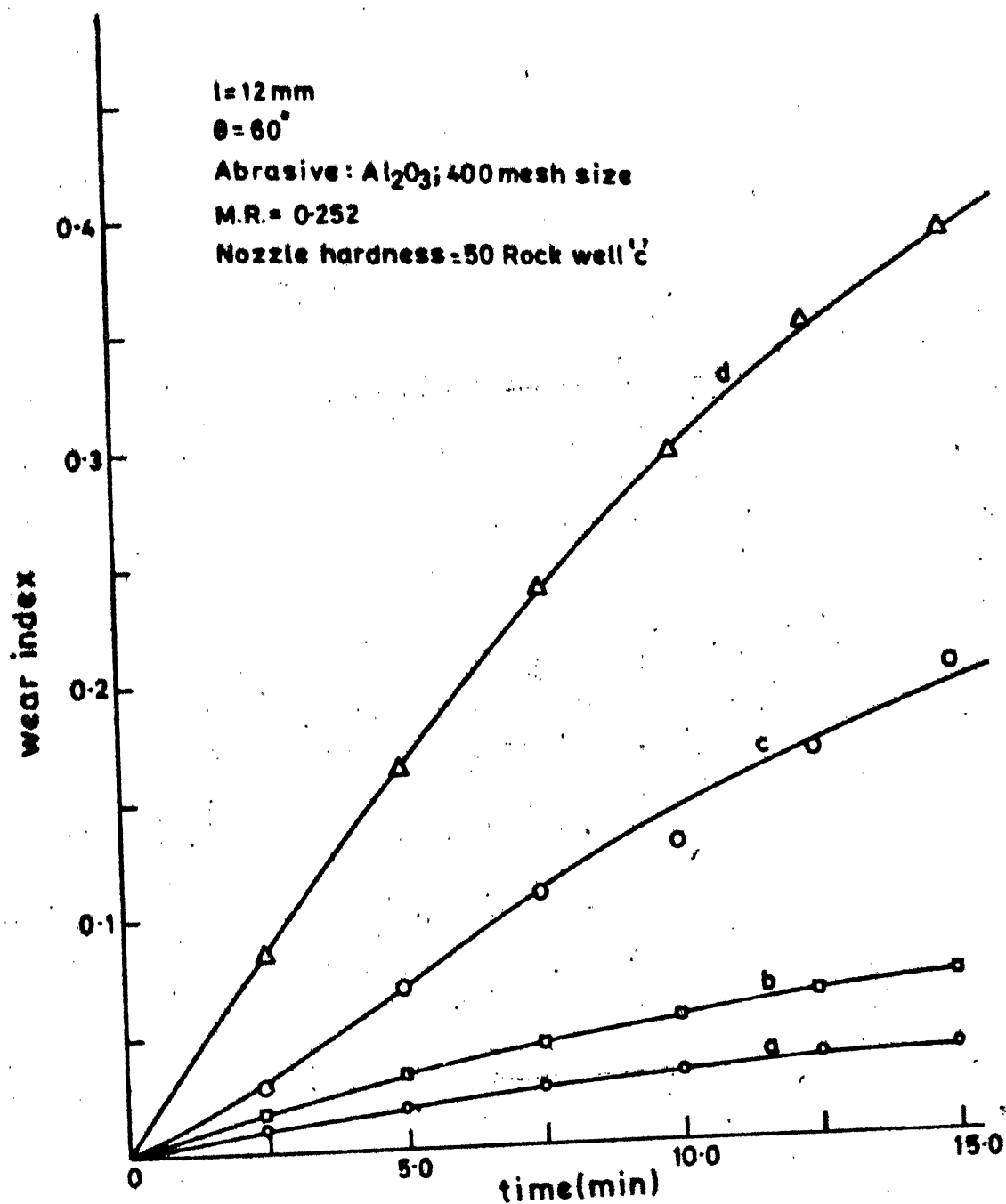


FIG.12 (a) VARIATION OF WEAR RATE WITH TIME FOR
 DIFFERENT NOZZLE DIAMETERS
 (a) 1.62mm (b) 1.17mm (c) 0.9mm (d) 0.8mm

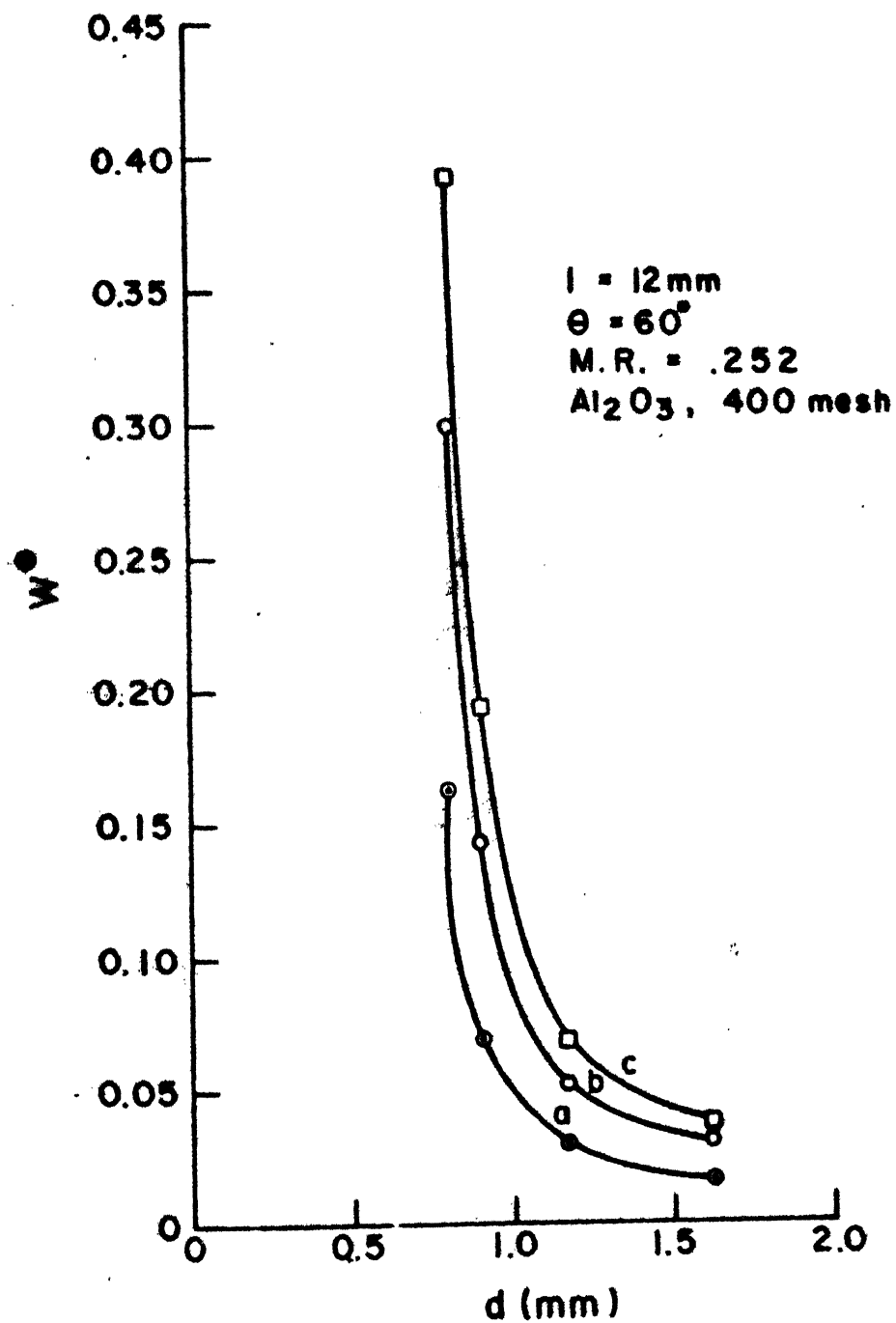


Fig. 12(b) Variation of wear index with nozzle diameter.
 (a) for 5 min., (b) for 10 min., (c) for 15 min.

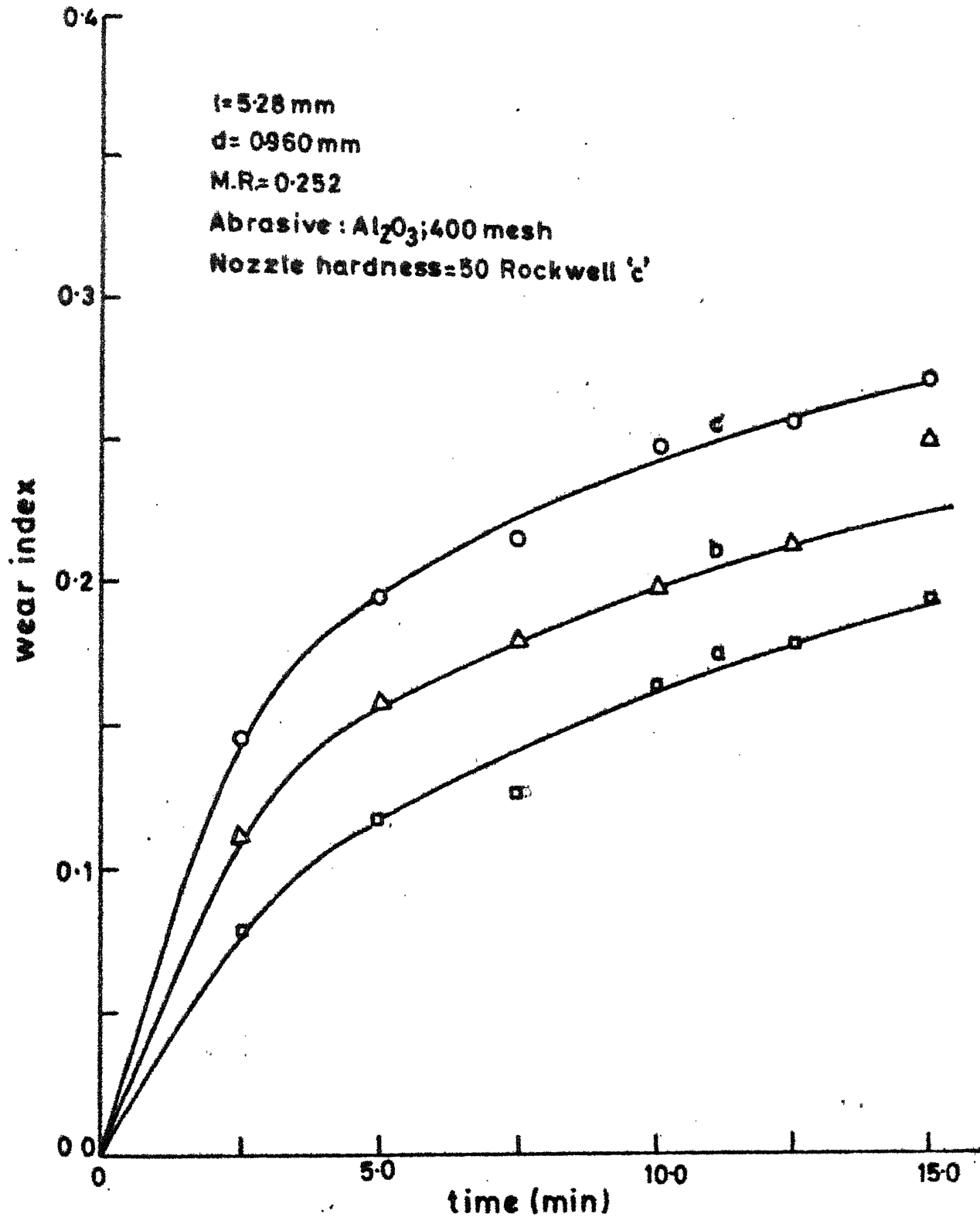


FIG.13 VARIATION OF WEAR INDEX WITH TIME FOR
 DIFFERENT NOZZLE ENTRANCE ANGLES
 (a) 120° (b) 90° (c) 60°

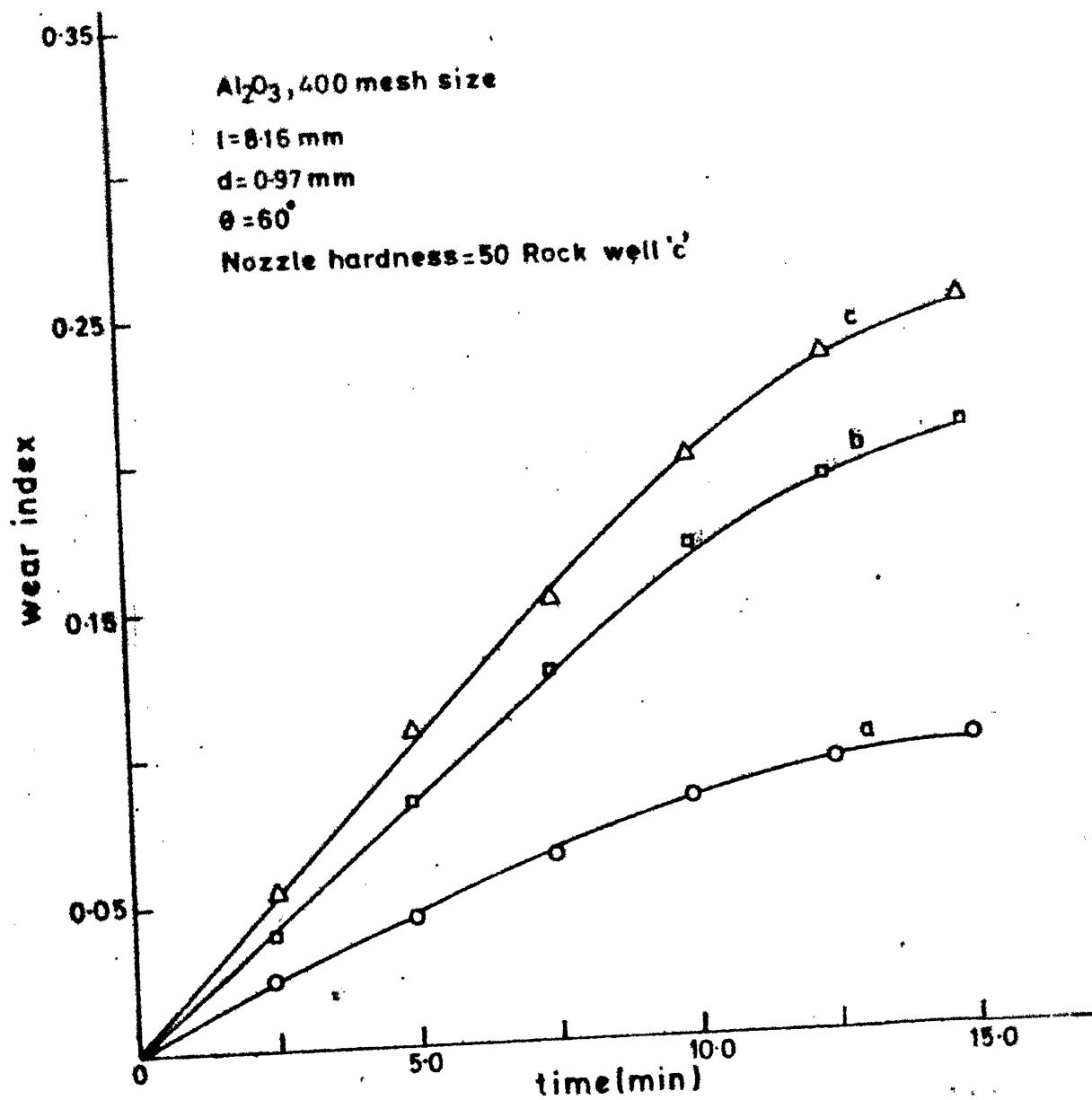


FIG-14(a) VARIATION OF WEAR INDEX WITH TIME FOR
DIFFERENT MIXTURE RATIOS
(a) 0.096 (b) 0.252 (c) 0.332

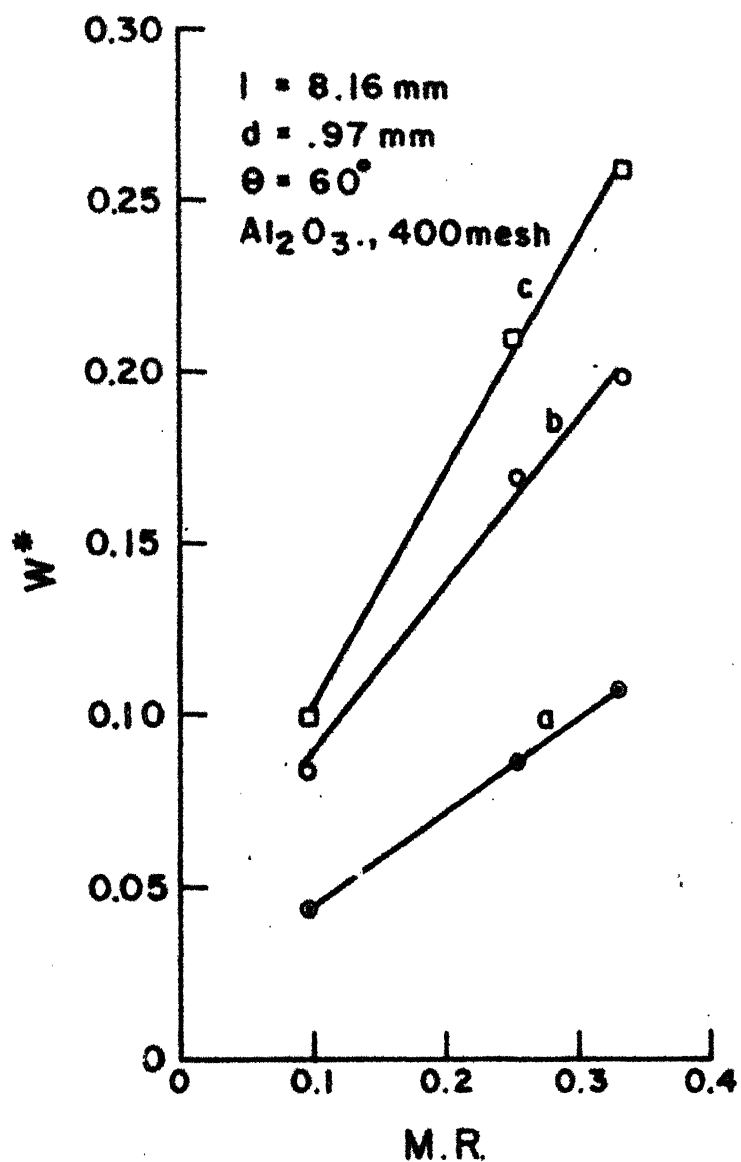


Fig. 14 b Variation of wear index with mixture ratio (a) for 5 min., (b) for 10 min., (c) for 15 min.

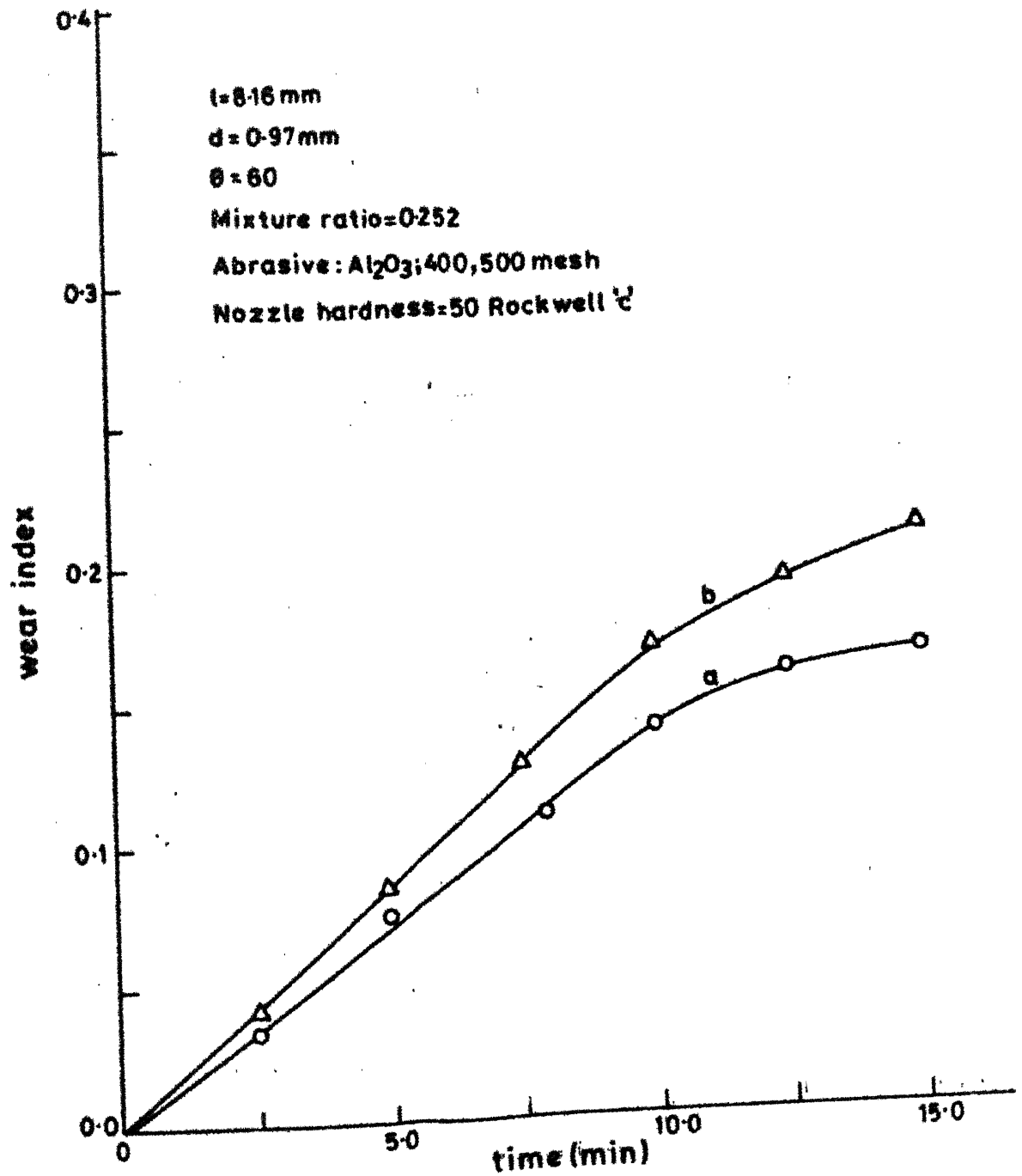


FIG.15 VARIATION OF WEAR INDEX WITH TIME FOR DIFFERENT MESH SIZE
(a) 500 mesh (b) 400 mesh

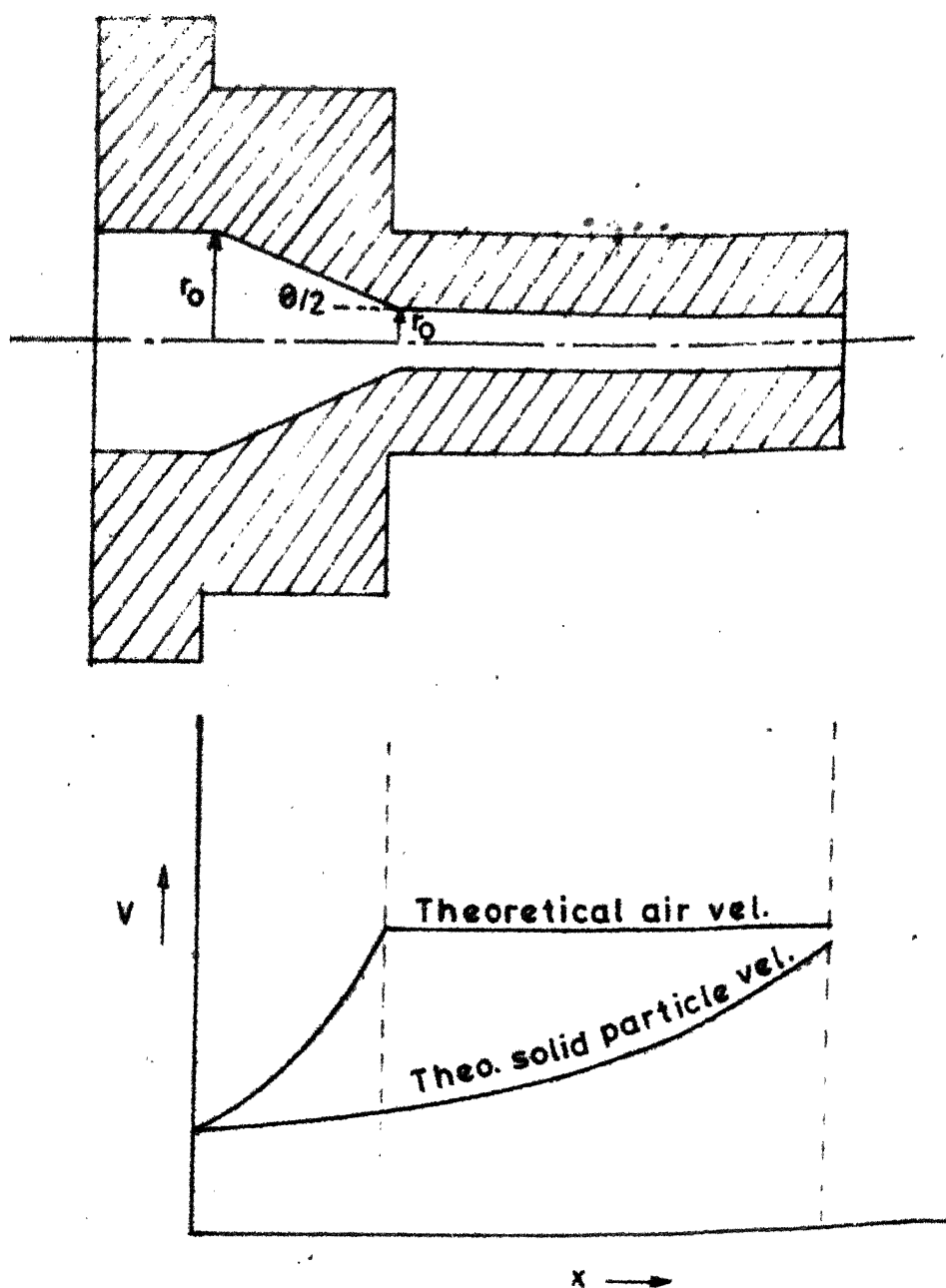


FIG-16 VELOCITY PROFILE INSIDE THE NOZZLE

CENTRAL LIBRARY
 I. I. T. Kanpur.
 Acc. No. A 82651